Highly Effective Photocatalytic Performance in Visible Light of Sodium Hexametaphosphate Capped Ni-Doped ZnO Nanoparticles

K. Mageswari[1,] , T. Bavani[2,] , J. Madhavan[2,] and P. Prabukanthan[1,*,]

[1]Materials Chemistry Lab, Department of Chemistry, Muthurangam Government Arts College, Vellore-632002, India
[2]Solar Energy Lab, Department of Chemistry, Thiruvalluvar University, Vellore-632115, India

*Corresponding author: Tel: +91 416 2262068; E-mail: pprabukanthan76@hotmail.com

This study describes the microwave assisted synthesis of without and with sodium hexametaphosphate (SHMP) (1 mol%) capped 3 mol% Ni-doped ZnO nanoparticles. Various sophisticated analytical techniques were used to characterize the Ni-doped ZnO nanoparticles. The results showed that including SHMP capped 3 mol% Ni-doped ZnO nanoparticles has a significant influence on the photocatalyst and structural characteristics of the ZnO nanoparticles. Under visible light illumination, SHMP capped 3 mol% Ni-doped ZnO nanoparticles demonstrated better photocatalytic degradation of methylene blue dye. As a result, SHMP capped 3 mol% Ni-doped ZnO nanoparticles synthesized are suitable materials for the environmental applications.

Keywords: Sodium hexametaphosphate, ZnO, Nickel, Methylene blue dye, Photocatalytic activity.

INTRODUCTION

The majority of environmental hazards are associated with toxic and non-biodegradable waste products and these pollutants are causing different kinds of contamination, including air, water and soil pollution. However, water-soluble formulations are often considered to be the most hazardous due to their direct impact on living organisms [1]. Moreover, the utilization of natural pigments derived from wastewaters generated by the textile and other industries has played a vital role in facilitating this process. Many colours are generally harmless when used alone, but when combined with water, they quickly pollute waste water by producing very toxic chemicals [2]. In addition, large quantities of inorganic salts and azo dyes are used in the textile industries. In addition to the aesthetic problems, it demonstrates substantial amounts of biotoxicity and harmful consequences [3]. To eliminate the effluents that contain dye, numerous water purification techniques have been established, including chemical oxidation, biodegradation, coagulation and flocculation, improved oxidation processes and photocatalyst [4].

In order to address a multitude of aquatic environmental pollution challenges, there has recently been a significant increase in demand for photocatalytic devices, which decomposes the organic pollutants into the simple inorganic components [5]. As a result, nanomaterials of metal oxide are attracting interest owing to the intriguing features as well as potential applications in a variety of key fields like environmental remediation, biomedicine, *etc*. Overall, the shape and size of these materials have a significant impact on their properties [6,7]. Studies on photocatalysis materials including TiO_2, $R-Fe_2O_3$, $SrTiO_3$, CdS, WO_3, ZnS and ZnO have potential to function as photocatalysts for a variety of applications [8]. Along with its higher quantum efficiency, ZnO is thought to be more efficient in photocatalytic performance than TiO_2 in various applications. Although ZnO exhibits significant photocatalytic properties, its catalytic efficiency is hindered by its wide band gap. Additionally, the photocatalytic activity of ZnO is limited to specific portions of the photon spectrum [9]. As a result of their substantial absorption in the visible range, transition-metals pollutants might extend photocatalytic efficiency through the visible wavelengths within the frequency and increase sensing applications of the component.

However, it is already reported that ZnO is a semiconductor of n-type photocatalyst with a band gap value of energy $E_g = \sim 2.9$ to 3.3 eV [10]. Although, it exhibits less visible absorption because of its broad band gap energy and only absorbing a

small portion in the solar spectrum. Additionally, the photo-catalytic degradation effectiveness of ZnO seems low within the visible spectrum due to which is quick replication for photo-excited e⁻/h⁺ couples [11]. A number of attempts have been successfully made to use ZnO a photocatalyst for organic pollutant the photodegradation [12]. However, no results that have been published so far on the use of a capping agent like sodium hexametaphosphate (SHMP) with Ni-doped zinc oxide for the degradation of organic colours.

Doping using different capping agents is one of the many ways that one can adjust the effectiveness of photocatalytic degradation to the transmission of charge between particles. Over the course of time, the utilization of ZnO as a capping material has witnessed significant advancements. Moreover, multiple types of different techniques for capping have been emerged and in most of the cases organic molecules have been employed as catalysts due to their ability to facilitate photo-degradation. Krishnan & Shriwastav [13] explored the use of chlorophyll influenced TiO₂ (chl/TiO₂) nanoparticles in visible light photocatalytic methylene blue degradation using blue LED irradiation. Under the optimal conditions, 85% of degradation was attained after 2 h of visible blue LED irradiation. Simiarly, Belachew *et al.* [14] developed a reduced graphene oxide grafted Ag/ZnO (rGO-Ag/ZnO) nanocomposite with L-methionine (L-Met) for the synergetic photocatalytic degra-dation of methylene blue dye upto 85%.

In the current study, the microwave irradiation process using SHMP (1 mol%) capped with 3 mol% Ni doped ZnO nanoparticles. The selectively chosen 3 mol% Ni doped ZnO [15] capped with SHMP shown here has a greater capacity for photocatalytic destruction of the target pollutant. The photo-catalytic activity of SHMP capped with 3 mol% Ni doped ZnO nanoparticles was investigated using the degradation of methy-lene blue dye according to visible light illumination. The possi-bility of a reaction mechanism between SHMP capped with 3 mol% Ni doped ZnO nanoparticles using the methylene blue dye degradation process under visible light irradiation is investigated.

EXPERIMENTAL

All the chemicals and reagents were utilized without further any purification. Sigma-Aldrich provided zinc nitrate, nickel (II) nitrate, sodium hexametaphosopate (SHMP), methylene blue and sodium hydroxide.

Synthesis of 3 mol% Ni doped ZnO and SHMP capped Ni doped ZnO nanoparticles: Zinc nitrate with nickel(II) nitrate concentration 3 mol% was prepared *via* the microwave irradiation technique [16]. The method described above was used to prepare SHMP 1 mol% capped Ni doped ZnO nano-particles within with a mixture of zinc nitrate and nickel nitrate.

Characterization: The samples used in this investigation were characterized using an X-ray diffractometer. The Cu*K*α radiation (λ = 1.5406 Å) produced the X-rays and the diffra-ction patterns were detected in the 2θ range between 10º and 80º with a step size of 0.02º. Fourier transformation spectro-meter Spectrum 2000, manufactured by Perkin-Elmer, was used to examine the chemical compounds of synthesized without

SHMP 3 mol% Ni doped ZnO nanomaterials and with SHMP 3 mol% Ni doped ZnO nanomaterials. The HRTEM images of synthesized photocatalysts were obtained with a JEOL-Jem 2100 apparatus to characterize specimens from the current study.

Photodegradation studies: The photocatalytic degradation of methylene blue dye solution within visible light irradiation was used to evaluate the photocatalytic efficacy of the prepared nanoparticles. The source of the radiation was tungsten halogen lamp with a power output of 250 W. A 75 mg of catalyst was introduced to 75 mL of methylene blue dye solution (2×10^{-5} M) in a cylindrical glass jar in a conventional photocatalytic degradation experiment. In order to attain a equilibrium through sorption, the suspension underwent magnetic agitation for a duration of 45 min in absence of light. A 5 mL of suspension was taken and centrifuged on a regular basis to produce the supernatant solution. Using a JASCO V-630 (Japan) UV-visible spectrophotometer, the remainder of the solution was subjected to an estimation of the maximum absorption at (λ_{max}) 664 nm.

The photocatalytic degradation percentage (%) was calcul-ated using eqn. 1:

$$D\ (\%) = \frac{C_o - C}{C_o} \times 100 \tag{1}$$

where C_o is the initial dye concentration and C is the concen-tration of the dye after regular illumination times.

RESULTS AND DISCUSSION

X-ray diffraction studies: Fig. 1 displayed the results of an XRD analysis performed on 3 mol% Ni doped ZnO nano-particles, comparing samples with and without SHMP capping. The synthesized 3 mol% Ni doped ZnO nanoparticles exhibited all the major peaks observed in the ZnO nanoparticles, which were ascribed to the (200) diffraction plane of nickel (JCPDS No. 001-1239). The observed result can be attributed to the successful integration of nickel atoms within the hexagonal
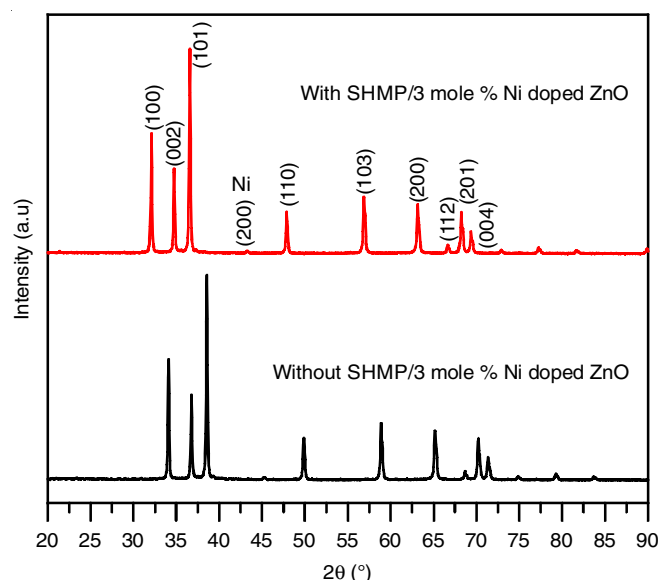

Fig. 1.   XRD pattern of without SHMP capped 3 mol% Ni doped ZnO and with SHMP capped 3 mol% Ni doped ZnO nanoparticles

lattice of the ZnO material. This integration is specifically associated with the (200) diffraction plane of nickel as indicated by the JCPDS card No. 001-1239. Furthermore, the XRD spectrum of 3 mol% Ni doped ZnO nanoparticles by SHMP caps exhibits more pronounced shoulder features compared to the without SHMP-capped 3 mol% Ni doped ZnO nanoparticles counterparts [17]. This observation implies a higher occurrence of peak defects, which can be attributed to structural flaws such as irregularities in size and shape. Furthermore, the XRD pattern of the with SHMP-capped 3 mol% Ni doped ZnO nanoparticles displays lower 2θ values in contrast to the pattern of the uncapped ZnO nanoparticles. This observation might signify the influence of stress induced by SHMP binding to the surfaces of the nanoparticles [18].

FT-IR studies: Fig. 2a illustrates the FTIR spectra of 3 mol% Ni-doped ZnO nanoparticles with and without SHMP capping. The spectrum reveals the distinctive peaks attributed to various functional groups, including ZnO and Ni stretching and bending vibrations, within the spectral range of 1433 to 3461 cm^{-1} as well as 2426, 1158 and 565 cm^{-1}, respectively. The FT-IR analysis of the SHMP-capped 3 mol% Ni-doped ZnO nanoparticles indicates key shifts in bands at different wavenumbers. The observed shifts in the spectra indicate the presence of additional functional groups, namely the phosphate (–P=O) group, which is detected within the range of 1180 cm^{-1} and the P-O-P group, which appears at approximately 870 cm^{-1} (Fig. 2b).

Photoelectrochemical studies: The photocurrent behaviour of without SHMP capped 3 mol% Ni doped ZnO and with SHMP capped 3 mol% Ni doped ZnO a nanoparticle with three on-off cycles is depicted in Fig. 3a. The photocurrent performance of the with SHMP capped 3 mol% Ni doped ZnO was superior than that of the without SHMP capped 3 mol% Ni doped ZnO, indicating an improvement in charge-separation efficiency [19]. The electrochemical impedance spectroscopy (EIS) was used to measure the interfacial charge transfer (CT)
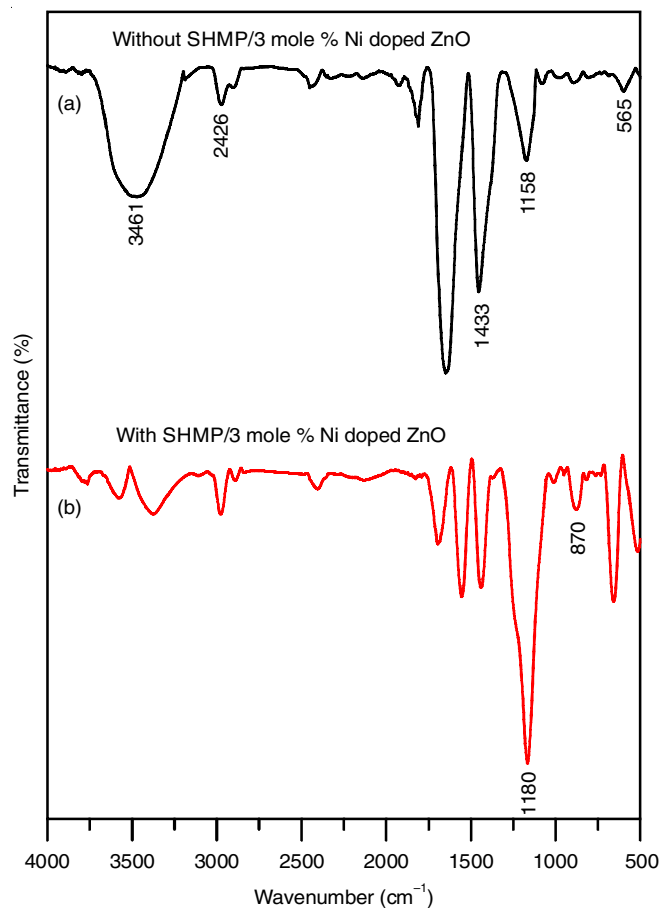
Fig. 2. FT-IR analysis of without SHMP capped 3 mol% Ni doped ZnO and with SHMP capped 3 mol% Ni doped ZnO nanoparticles

rate of without SHMP capped 3 mol% Ni doped ZnO and with SHMP capped 3 mol% Ni doped ZnO nanoparticles and the conforming Nyquist plots are presented in Fig. 3b. The semi-circular radius of with SHMP capped 3 mol% Ni doped ZnO photocatalyst is lower.
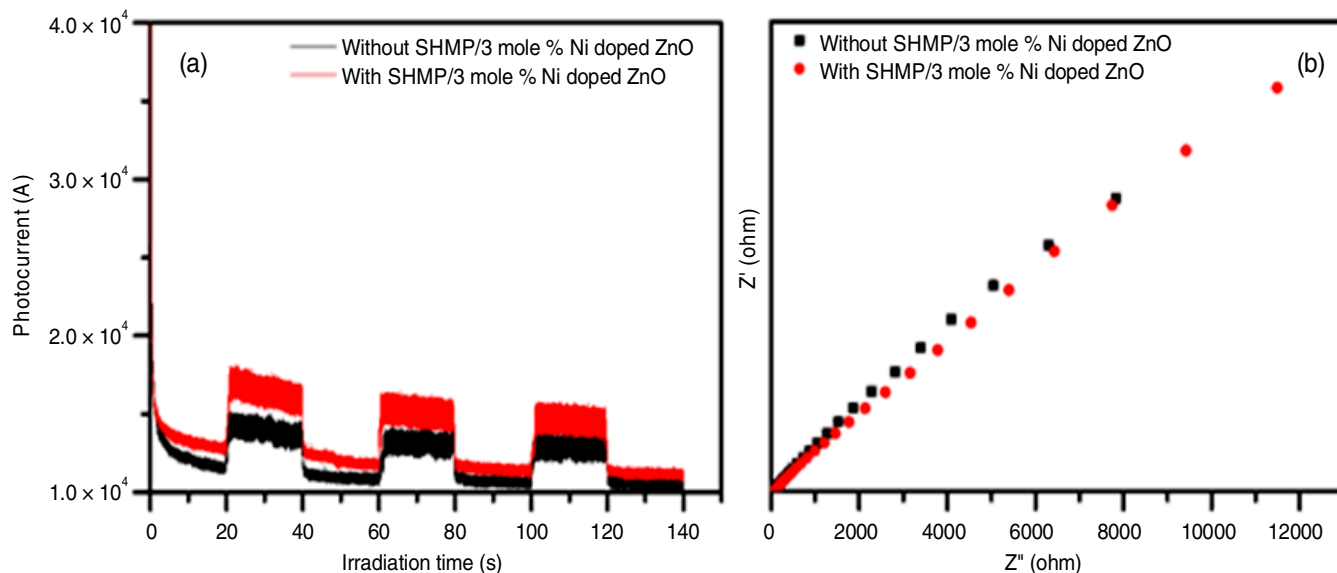
Fig. 3. (a) Transient-photocurrent curves (b) Nyquist plots of the without SHMP capped 3 mol% Ni doped ZnO and with SHMP capped 3 mol% Ni doped ZnO nanoparticle photocatalysts
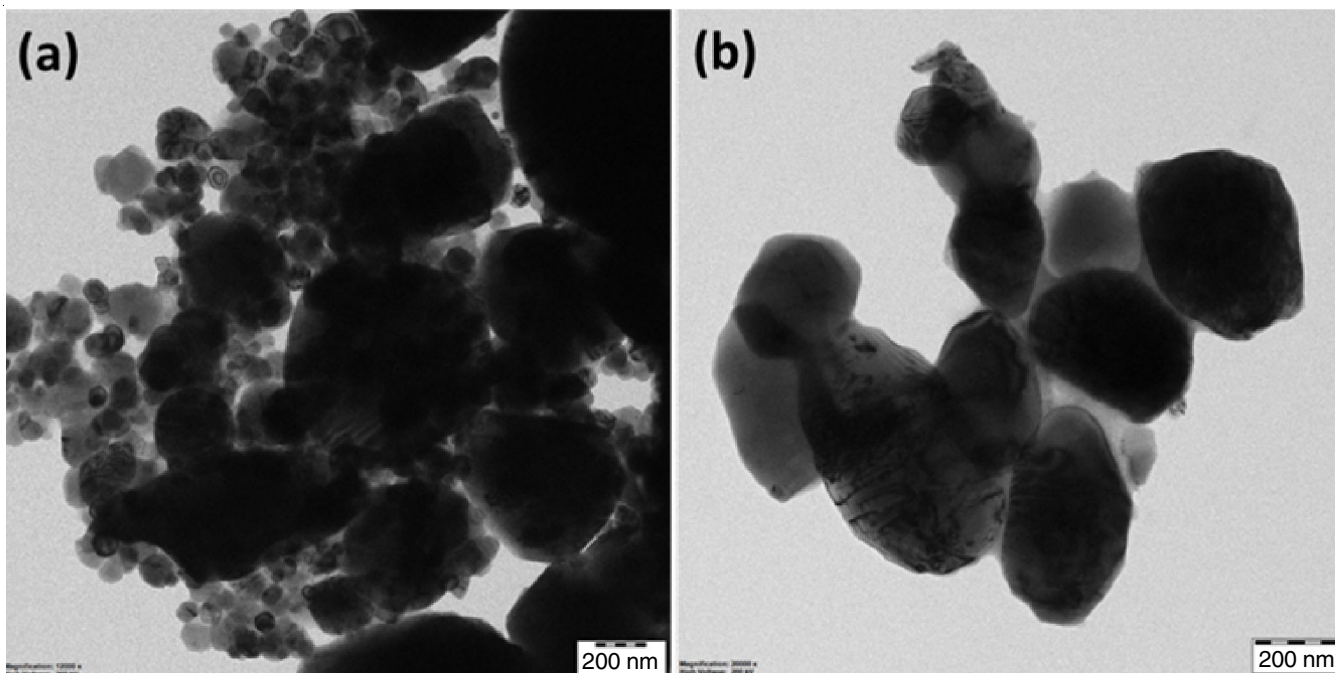
Fig. 4. TEM images of (a) without and (b) with SHMP capped 3 mol% Ni doped ZnO nanoparticles

Morphological studies: The HRTEM analysis was conducted to examine the surface morphology of without SHMP capped 3 mol% Ni doped ZnO and with SHMP capped 3 mol% Ni doped ZnO nanoparticles. When compared to without SHMP capped 3 mol% Ni doped ZnO nanoparticles, without SHMP capped 3 mol% Ni doped ZnO was found to have a heavily agglomerated surface and a spherical structure, as shown in Fig. 4. The SHMP capped 3 mol% Ni doped ZnO nanoparticles exhibited a lower degree of agglomeration compared to the undoped ZnO nanoparticles. This observation suggests that the presence of 3 mol% Ni doped concentrations has a slight influence on the size, shape and aggregation of ZnO nanoparticles. The Ni doped ZnO nanoparticles with a SHMP capped and a 3 mol% Ni content have a reduced size [20].

The nanoparticles with SHMP capped were identified by their elementary composition using the energy dispersive X-ray investigation. The EDX patterns of the SHMP capped 3 mol% Ni doped ZnO nanoparticles are shown in Fig. 5. The spectrum shows that there are no additional signals present and only the peaks due to the elements zinc (Zn), oxygen (O),
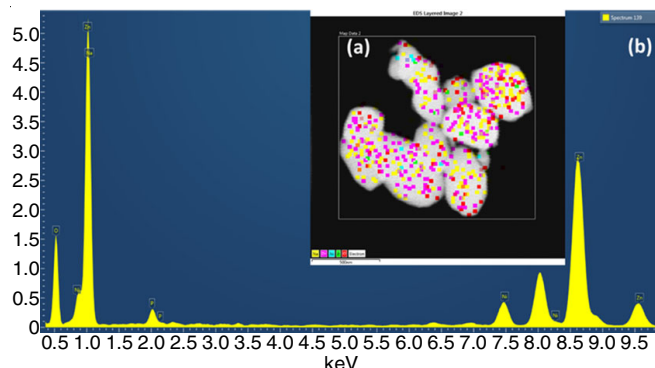

Fig. 5.   (a) EDX and (b) elemental mapping spectrum of with SHMP capped 3 mol% Ni doped ZnO nanoparticles

sodium (Na), phosphorus (P) and nickel (Ni) are present. This indicates that the Ni-doped SHMP capped ZnO nanoparticles are confirmed. The exhbits of Zn, O, P, Na and Ni elements is confirmed by the EDX spectrum of SHMP capped 3 mol% Ni doped ZnO nanoparticles.

Photocatalytic degradation studies: The photocatalytic degradation capacity of without SHMP capped 3 mol% Ni doped ZnO and with SHMP capped 3 mol% doped ZnO nanoparticles has been assessed using under visible light irradiation by methylene blue dye. It was found that SHMP capped 3 mol% Ni doped ZnO nanoparticle exhibited an 85% efficiency in degrading methylene blue compared to without SHMP capped 3 mol% Ni doped ZnO, respectively (Fig. 6). The reason is attributed due to the activation of surface sites for methylene blue dye adsorption for photodegradation for better efficiency in cased of SHMP capped 3 mol% Ni doped ZnO nanoparticle [21,22].

Reusability studies: Fig. 7. Illutrates that the recycling analysis of with SHMP capped 3 mol% Ni doped ZnO nanoparticle towards the breakdown of the pollutant when exposed to the visible light. The catalyst was retrieved after each run, properly rinsed in water and then dried at 70-80 ºC for 3 h before being reintroduced in the following run. Additionally, it was assumed that the photocatalytic activity of SHMP capped 3 mol% Ni doped ZnO nanoparticles was almost unchanged after three runs. The XRD and TEM images was reused photocatalyst samples are shown in Fig. 7b and 7c. From Fig. 7b, it is revealed that the SHMP capped 3 mol% Ni doped ZnO nanoparticle photocatalyst even after recycling process both the XRD crystalline phases and the structural morphology has no considerable change. Thus, the results above clearly show that the SHMP capped 3 mol% Ni doped ZnO nanoparticles have better photostability and reusability characteristics, making them an ideal material for wastewater treatment.
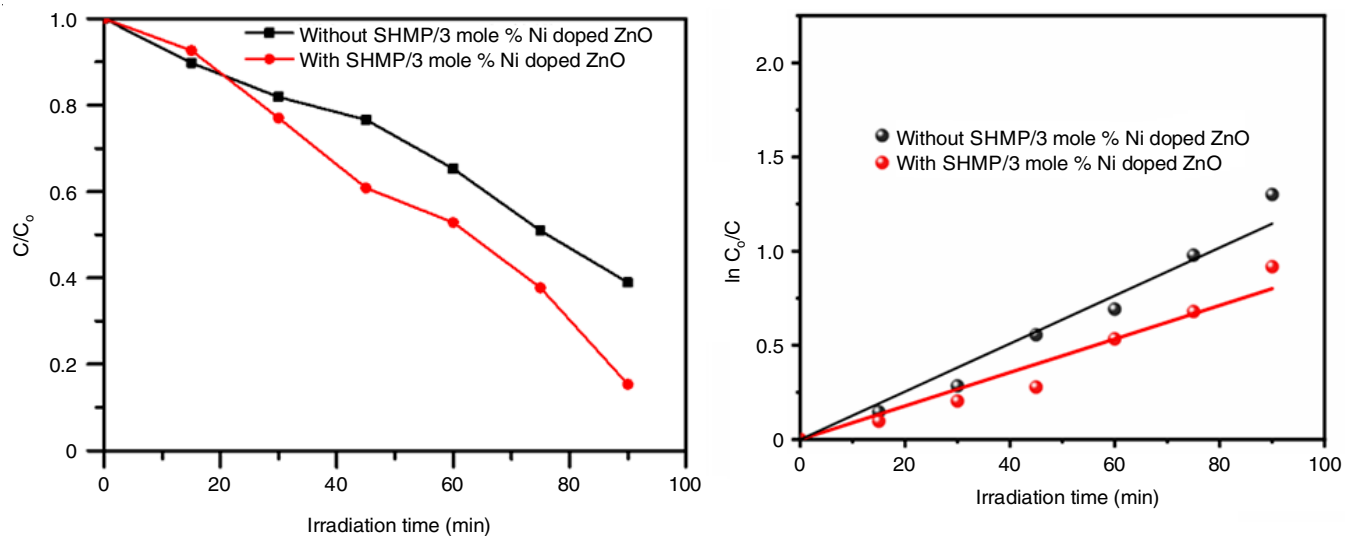
Fig. 6. Photocatalytic activity of without SHMP capped 3 mol% Ni doped ZnO and with SHMP capped 3 mol% Ni doped ZnO
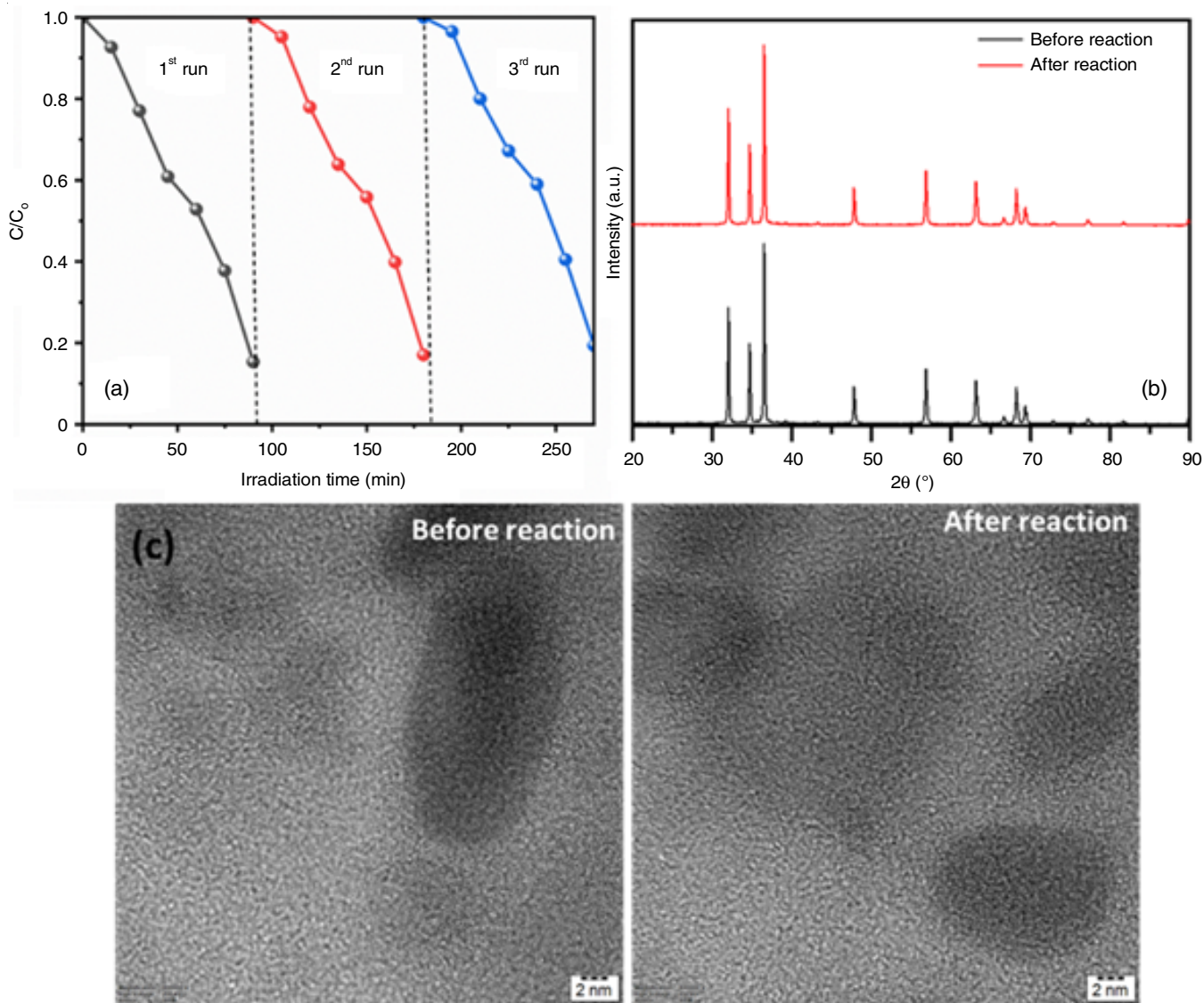

Fig. 7. (a) Recycling test results for photocatalytic degradation of methylene blue in VLI using SHMP-capped 3 mol% Ni doped ZnO nanoparticles (b) XRD patterns and (c) TEM images of before and after recycling test of with SHMP capped 3 mol% Ni doped ZnO nanoparticle

Photocatalyst mechanism: The hypothesized method for the degradation of methylene blue dye by SHMP capped 3 mol% Ni doped ZnO nanoparticles is illustrated in Fig. 8. A specified number of electrons (e^-) and holes are produced during the ZnO nucleation process. Recombination is hindered by Ni because they absorb the excess electrons of generatred ZnO. The superoxide radical is created as a result of an interaction between the e^- and O_2 [23]. For instance, 85% of methylene blue can be eliminated in 90 minutes by employing with SHMP-capped, 3 mol% Ni-doped ZnO nanoparticles. The objective was achieved through the exposure of the material to visible light. This could be the result of hydroxyl radicals ($OH^•$) being produced when superoxide radicals interact with water molecules. The $OH^•$ and $O_2^{•-}$ that are created react with the methylene blue dye to fragment it into tiny pieces [20]. A greater synergistic effect of Ni-doped and SHMP for the formation of photocatalyst may also be the cause of SHMP:Ni:ZnO photocatalyst raising the degradation rate and enhancing the photocatalytic activity [24,25].
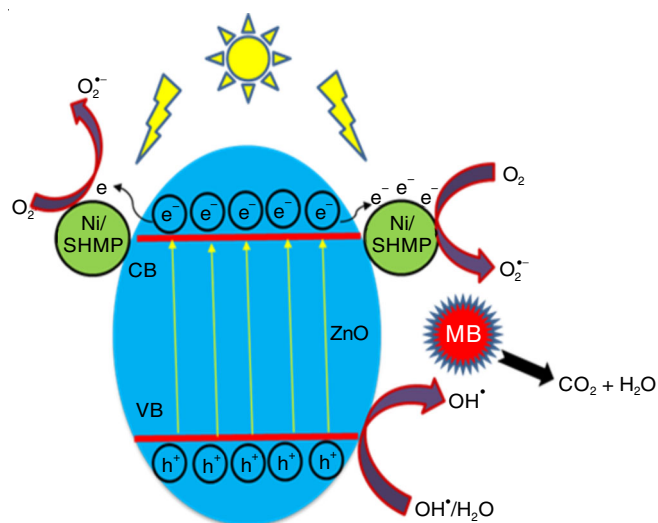

Fig. 8.   Schematic representation of photocatalytic degradation reaction mechanism towards degradation of methylene blue over with SHMP capped 3 mol% Ni doped ZnO nanoparticles under visible irradiation

Comparative studies: The SHMP/ZnO nanoparticle demonstrated higher photocatalytic activity when compared to the other ZnO catalysts towards the degradation of different compounds and dyes as mentioned in Table-1.

Conclusion

In this study, the synthesis and characterization of nanoparticles consisting of 3 mol% Ni-doped ZnO, both with and without SHMP capping, were conducted. Microwave irradiation was utilized as the chosen synthesis method. The synthesized materials were thoroughly analyzed using several techniques such as XRD, FT-IR, TEM and EDX. The EDX studies provided conclusive evidence that the SHMP were effectively and uniformly capped into the 3 mol% Ni doped ZnO compound, indicating the introduction of SHMP into the 3 mol% doped ZnO structure. The enhancement of the photocatalytic efficiency of material when compared to without SHMP capped 3 mol% Ni doped ZnO, with SHMP capped 3 mol% Ni doped ZnO nanoparticles exhibited superior degradation efficiency, particularly in the context of photocatalytic degradation. Among the various compositions, the nanoparticles with SHMP capped 3 mol% Ni doped ZnO demonstrated the most promising results in terms of photocatalytic performance. Specifically, with SHMP capped 3 mol% Ni doped ZnO nanoparticles exhibited an impressive 85% degradation efficiency in the photodegradation of methylene blue dye when irradiated with under visible light for 90 min. Based on these findings, the researchers concluded with SHMP capped 3 mol% Ni doped ZnO nanoparticles could be considered a highly effective and stable material for environmental remediation purposes, particularly in the context of photodegradation of methylene blue dye.

REFERENCES

1. M.V. Encinas, A.M. Rufs, M.G. Neumann and C.M. Previtali, *Polymer*, **37**, 1395 (1996);
    https://doi.org/10.1016/0032-3861(96)81137-2
2. H.R. Pouretedal and M.H. Keshavarz, *Int. J. Phys. Sci.*, **6**, 6268 (2011);
    https://doi.org/10.5897/IJPS09.251
3. I. Akanyeti, A. Kraft and M.C. Ferrari, *J. Water Process Eng.*, **17**, 102 (2017);
    https://doi.org/10.1016/j.jwpe.2017.02.014
4. A. Ahmad, S.H. Mohd-Setapar, C.S. Chuong, A. Khatoon, W.A. Wani, R. Kumar and M. Rafatullah, *RSC Adv.*, **5**, 30801 (2015);
    https://doi.org/10.1039/C4RA16959J
5. M. Jothibas, C. Manoharan, S.J. Jeyakumar, P. Praveen, I. Kartharinal Punithavathy and J.P. Richard, *J. Solar Energy*, **159**, 434 (2018);
    https://doi.org/10.1016/j.solener.2017.10.055

TABLE-1
A COMPARISON OF SEVERAL ZnO NANOPARTICLE PHOTOCATALYSTS FOR THE DEGRADATION
OF VARIOUS ORGANIC MATERIALS UNDER VARIOUS EXPERIMENTS CONDITIONS

Photocatalysts	Pollutants	Photocatalytics performance (%)	Irradiation time (min)	Ref.
Gold decorated ZnO	Rhodamine B	95.00	60	[26]
Ni-doped ZnO	4-Nitrophenol	83.00	120	[27]
ZnFe$_2$O$_4$@ZnO	Rhodamine B	91.87	240	[28]
Ag/ZnO	Methylene blue	76.00	240	[29]
CeO$_2$/ZnO@ZnS	*p*-Nitrophenol	97.00	25	[30]
S-doped ZnO	Resorcinol	~100.00	420	[31]
Pithecellobium dulce/ZnO	Methylene blue	63.00	120	[32]
ZnO/CdS	Reactive red 141	73.00	240	[33]
SHMP capped Ni doped ZnO	Methylene blue	85.00	90	This work

6. A. Mclaren, T. Valdes-Solis, G. Li and S.C. Tsang, *J. Am. Chem. Soc.*, **131**, 12540 (2009);
    https://doi.org/10.1021/ja9052703

7. N.M. Flores, U. Pal, R. Galeazzi and A. Sandoval, *RSC Adv.*, **4**, 41099 (2014);
    https://doi.org/10.1039/C4RA04522J

8. L-L. Lin, X.-G Wang and J. Zhang, eds. H. Haeri: A Review on the Application of Photocatalytic Materials, In: Materials in Environmental Engineering: Proceedings of the 4th Annual International Conference on Materials Science and Environmental Engineering, Berlin, Boston: De Gruyter, pp. 473-480 (2017);
    https://doi.org/10.1515/9783110516623-046

9. M.Y. Chiang and H.N. Lin, *Mater. Lett.*, **160**, 440 (2015);
    https://doi.org/10.1016/j.matlet.2015.08.021

10. A. Murali, P.K. Sarswat and H.Y. Sohn, *Mater. Today Chem.*, **11**, 60 (2019);
    https://doi.org/10.1016/j.mtchem.2018.10.007

11. M. Samadi, M. Zirak, A. Naseri, E. Khorashadizade and A.Z. Moshfegh, *Thin Solid Films*, **605**, 2 (2016);
    https://doi.org/10.1016/j.tsf.2015.12.064

12. K. Bhuvaneswari, G. Palanisamy, K. Sivashanmugan, T. Pazhanivel and T.J. Maiyalagan, *J. Environ. Chem. Eng.*, **9**, 104909 (2021);
    https://doi.org/10.1016/j.jece.2020.104909

13. S. Krishnan and A. Shriwastav, *J. Environ. Chem. Eng.*, **9**, 104699 (2021);
    https://doi.org/10.1016/j.jece.2020.104699

14. N. Belachew, M.H. Kahsay, A. Tadesse and K. Basavaiah, *J. Environ. Chem. Eng.*, **8**, 104106 (2020);
    https://doi.org/10.1016/j.jece.2020.104106

15. A.I. Yalçin and F.G. Yazicioglu, *J. Exercise Ther. Rehab.*, **10**, 1 (2023);
    https://doi.org/10.15437/jetr.1133913

16. K. Mageswari, P. Prabukanthan and J. Madhavan, *Environ. Sci. Pollut. Res. Int.*, **30**, 40174 (2023);
    https://doi.org/10.1007/s11356-022-25097-9

17. R. Mohan, C. Rakkappan, N. Punitha, K. Jayamoorthy, P. Magesan and N. Srinivasan, *Chemical Physics Impact*, **7**, 100260 (2023);
    https://doi.org/10.1016/j.chphi.2023.100260

18. K.F. Chepape, T. P. Mofokeng, P. Nyamukamba, K.P. Mubiayi, and M.J. Moloto, *J. Nanotechnol.*, **2017**, 5340784 (2017);
    https://doi.org/10.1155/2017/5340784

19. B. Fang, Z. Xing, D. Sun, Z. Li and W. Zhou, *Adv. Powder Mater.*, **1**, 100021 (2022);
    https://doi.org/10.1016/j.apmate.2021.11.008

20. S. Arumugam, T. Bavani, M. Preeyanghaa, S.O. Alaswad, B. Neppolian, J. Madhavan and S. Murugesan, *Chemosphere*, **308**, 136100 (2022);
    https://doi.org/10.1016/j.chemosphere.2022.136100

21. P. Pascariu, I.V. Tudose, M. Suchea, E. Koudoumas, N. Fifere and A. Airinei, *Appl. Surf. Sci.*, **448**, 481 (2018);
    https://doi.org/10.1016/j.apsusc.2018.04.124

22. M. Adeel, M. Saeed, I. Khan, M. Muneer and N. Akram, *ACS Omega*, **6**, 1426 (2021);
    https://doi.org/10.1021/acsomega.0c05092

23. S. Siahrostami, G.-L. Li, V. Viswanathan and J.K. Nørskov, *J. Phys. Chem. Lett.*, **8**, 1157 (2017);
    https://doi.org/10.1021/acs.jpclett.6b02924

24. S. Rajendran, M.M. Khan, F. Gracia, J. Qin, V.K. Gupta and S. Arumainathan, *Sci. Rep.*, **6**, 31641 (2016);
    https://doi.org/10.1038/srep31641

25. S. Vignesh, S. Suganthi, J.K. Sundar, V. Raj and P.I. Devi, *Appl. Surf. Sci.*, **479**, 914 (2019);
    https://doi.org/10.1016/j.apsusc.2019.02.064

26. A. Serra, Y. Zhang, B. Sepúlveda, E. Gómez, J. Nogués, J. Michler and L. Philippe, *Appl. Catal. B*, **248**, 129 (2019);
    https://doi.org/10.1016/j.apcatb.2019.02.017

27. M. Ahmad, W. Rehman, M.M. Khan, M.T. Qureshi, A. Gul, S. Haq, R. Ullah, A. Rab and F. Menaa, *J. Environ. Chem. Eng.*, **9**, 104725 (2021);
    https://doi.org/10.1016/j.jece.2020.104725

28. L.T. Nguyen, D.V.N. Vo, L.T. Nguyen, A.T. Duong, H.Q. Nguyen, N.M. Chu, D.T.C. Nguyen and T.V. Tran, *Environ. Technol. Innov.*, **25**, 102130 (2022);
    https://doi.org/10.1016/j.eti.2021.102130

29. M.F. Abdel Messih, M.A. Ahmed, A. Soltan and S.S. Anis, *J. Phys. Chem. Solids*, **135**, 109086 (2019);
    https://doi.org/10.1016/j.jpcs.2019.109086

30. X. Jiang, L. Huang, J. Li, L. Zhang, X. Guo, Y. Li and X. Sun, *J. Environ. Chem. Eng.*, **9**, 105608 (2021);
    https://doi.org/10.1016/j.jece.2021.105608

31. V. Kumari, A. Mittal, J. Jindal, S. Yadav and N. Kumar, *Front. Mater. Sci.*, **13**, 1 (2019);
    https://doi.org/10.1007/s11706-019-0453-4

32. G. Madhumitha, J. Fowsiya, N. Gupta, A. Kumar and M. Singh, *J. Phys. Chem. Solids*, **127**, 43 (2019);
    https://doi.org/10.1016/j.jpcs.2018.12.005

33. T. Senasu, T. Chankhanittha, K. Hemavibool and S. Nanan, *Mater. Sci. Semicond. Process.*, **123**, 105558 (2020);
    https://doi.org/10.1016/j.mssp.2020.105558